The Effect of Ti Content on α' Martensite Phase Transformation, and Magnetic Properties by Mössbauer Spectroscopy in Fe–30%Ni–x%Ti (wt%) Alloys

E. Yaşar[a], U. Erdem[b], M. Akif Tuna[c], O. Armağan[c] and T. Kirindi[d,*]

[a]Department of Physics, Science and Arts Faculty, Kırıkkale University, Yahsihan 71450, Kırıkkale, Turkey
[b]Scientific and Technological Research Laboratories, Kırıkkale University, Yahsihan 71450, Kırıkkale, Turkey
[c]Department of Physics, Kırıkkale University, Graduate School of Natural and Applied Science, Yahsihan 71450, Kırıkkale, Turkey
[d]Department of Mathematic and Science Education, Faculty of Education, Kırıkkale University, Yahsihan 71450, Kırıkkale, Turkey

(Received May 4, 2017; revised version August 17, 2017; in final form February 12, 2018)

In this study, the influence of Ti content on the microstructure of the martensite bcc α'), which was formed by thermal effect, was investigated by scanning electron microscope and transmission electron microscope observations, in Fe–30Ni–xTi (x = 0.8, 1.8, 2.6) alloys. The crystallographic orientation relationship between austenite fcc (γ) and thermally induced bcc (α') martensite was found to be as $(111)_\gamma//(011)_\alpha$ (Kurdjumov–Sachs (K–S)), by the electron diffraction analysis. The martensitic transformation temperature (M_s) of α' martensite was determined as –41 °C, –62 °C, and –76 °C in the alloys with 0.8%, 1.8%, and 2.6% Ti concentration, respectively. The Mössbauer spectrometer analysis has been revealed by a paramagnetic character for the austenite phase and magnetically order character for α' martensite phase. Hyperfine magnetic field, isomer shift and volume fractions of phases were determined by the Mössbauer spectroscopy.

DOI: 10.12693/APhysPolA.133.1165

PACS/topics: martensitic transformation, Mössbauer spectroscopy, isomer shift, internal magnetic field

1. Introduction

Martensite transformations are diffusionless, solid-to-solid phase transitions of crystal lattice in response to changes in temperature and applied stress. Martensite phase transformation occurs athermally, with rapid transformation during quenching; yet, it also occurs isothermally, with a slower transformation, when Fe-based alloys are kept at a constant temperature and external deformation is applied [1]. In addition to kinetic differences in the transformation, there are differences in morphologies of both martensite phases [2–4]. As one of the most important structural materials, martensite — its morphology and substructure in Fe–Ni alloys — has been investigated widely [5–8]. The addition of a third element (Si, Co, Mo, etc.) to Fe–Ni alloys significantly influences their several physical properties, such as martensitic transformation and magnetic properties. Adding a small amount of Si, Mo and Co in Fe–Ni-based alloys have changed martensite phases morphology, the amount of martensite phases rate, and magnetic properties [9–11].

There is a strong correlation between magnetic behaviour and austenite-martensite phase transformation. Many ferrous alloys and steels undergoing martensitic transformation are paramagnetic or ferromagnetic in the austenitic state, but they are all ferromagnetic (or antiferromagnetic) in $\alpha\prime$ martensitic state [1, 12–15]. The Mössbauer spectroscopy is known as one of the useful and most sensitive techniques to reveal the magnetic characteristics of the materials. Thanks to the Mössbauer spectroscopy, some parameters can be determined, such as the hyperfine magnetic field, the isomer shift values, and the volume fraction of the austenite and martensite phases [1, 9, 11]. A paramagnetic to antiferromagnetic ordering reaction might also occur upon cooling in both austenite and martensite phases of Fe-based alloys. Local coupling makes two contributions: one is from the local or inner s-electrons, which are polarized by the unpaired $3d$-electrons at the origin of the local atomic magnetic moment; the other is from the itinerant $4s$-conduction electrons, which are also polarized by the local unpaired $3d$-electrons. The increased magnetic field is related to an increased localization of the $3d$-electrons. Ti atoms cause a clear increase in the magnetic moments at Fe sites [16] and an increase in ^{57}Fe hyperfine magnetic field as Ti concentration increases [17]; then, the magnetic moments decrease.

The current study is concerned with the examination of thermal induced martensite formation with respect to transformation kinetics, existing martensite morphology, and martensite transformation temperatures (M_s), as well as magnetic properties in Fe–30%Ni–x%Ti (x = 0.8, 1.8, and 2.6) alloys. Particularly, the magnetic properties of γ–α' martensitic transformation in these alloys were not examined by the Mössbauer spectroscopy technique.

*corresponding author; e-mail: talipkirindi@yahoo.com

2. Experimental

Fe–30%Ni–x%Ti (x = 0.8, 1.8, and 2.6) alloys were prepared by using the arc melting technique. After austenization at 1100 °C for 12 h in an evacuated silica capsule, specimens were quenched in water at room temperature. The austenite phase samples were transformed athermally in liquid nitrogen by holding them until their temperature reached the temperature of the liquid nitrogen; then, the samples were immediately transferred to boiling water to suppress the isothermal transformation. Finally, all samples were polished using a conventional mechanical polishing procedure. The etching reagent used to clarify the microstructures was a chemical solution containing 80 ml H_2O_2, 5 ml HF, and 15 ml H_2O. Microstructural characterizations were carried out using a JEOL JSM-5600 SEM operated at 20 kV. Foil samples under TEM observation were prepared from 3 mm discs and electropolished by using a double-jet polishing technique with a solution of 150 ml 2-butoxy ethanol, 5 ml perchloric acid, and 300 ml ethanol, at 35–40 V (dc) and at room temperature. Then, they were examined with a JEOL JEM-3010 TEM operated at 300 kV. Foil specimens (50 μm thick) were prepared using mechanical and chemical thinning procedures. The Mössbauer spectroscopy was carried out at room temperature by using a 50 mCi ^{57}Co source diffused in Rh. A Normos-90 computer program was used to find out the Mössbauer parameters and relative volume fractions of the austenite and martensite phases. To determine the M_s temperature of the homogenized transformation samples, we prepared the samples from 3 mm discs and encapsulated them in aluminium pans. Differential scanning calorimeter (DSC) measurements of this alloy were performed using a PerkinElmer Sapphire model thermal analysis, and measurements were taken at a cooling rate of 10 °C/min between 20 °C and –130 °C.

3. Results and discussion

3.1. The SEM observation

Analysis of SEM microstructures show that only lenticular athermal $\alpha\prime$-martensite morphology occurred in Fe–30%Ni–x%Ti alloys. In Fig. 1a–c SEM images illustrate that fcc (γ) to both bcc ($\alpha\prime$)-martensite transformation were a result of heat treatment in Fe–30%Ni–x%Ti alloys. Especially, quite large $\alpha\prime$ martensite crystals with quite large and shaped ridges regions are marked in austenite grain in Fe–30%Ni–0.8%Ti alloy (see Fig. 1a). In Fig. 1b, the martensite/austenite (M/A) interface of lenticular martensite is smoothly curved and the midrib region, where the martensitic transformation is thought to begin, has a substructure of fine transformation twins [2]. The small lenticular martensite partially fills the inside of the austenite grains in Fig. 1c. The SEM analysis observed that the size of the lenticular of $\alpha\prime$ martensite decreased with increased rate of Ti in Fe–30%Ni–x%Ti alloys (the lenticular martensite average lengths were measured as 50, 35, and 30 μm for x = 0.8%, 1.8%, and 2.6% Ti, respectively).

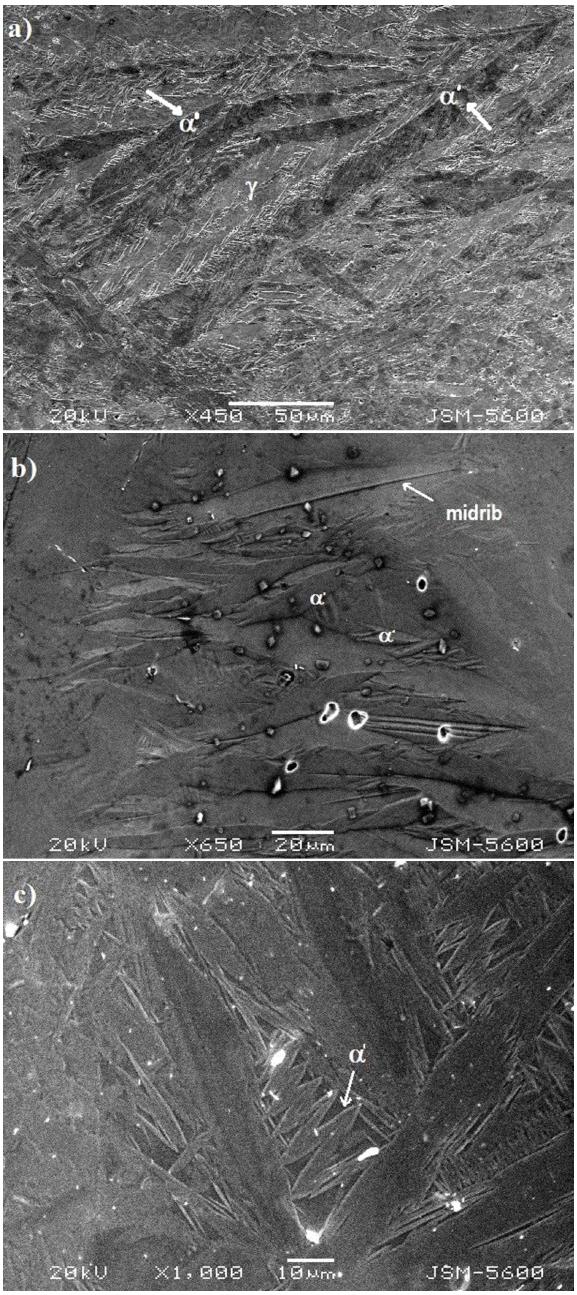

Fig. 1. SEM micrographs showing the microstructure of lenticular martensite: (a) Fe–30%Ni–0.8%Ti alloy, (b) Fe–30%Ni–1.8%Ti alloy and (c) Fe–30%Ni–2.6%Ti alloy.

3.2. The TEM observation and analysis

$\alpha\prime$ martensite and γ austenite phases' microstructures and electron diffraction pattern of these phases which marked region in micrographs were illustrated by Fig. 2a–c. Figure 2a illustrates the bright field TEM micrograph and the corresponding electron diffraction pattern of the Fe–30%Ni–0.8%Ti alloy lenticular martensite with a high dislocation density formed at –41 °C. Figure 2a shows the selected area diffraction pattern of austenite–martensite interface with $(1\text{–}1\text{–}1)_\gamma // (\text{–}110)_{\alpha'}$ and $[\text{–}101]_\gamma // [\text{–}1\text{–}11]_{\alpha'}$

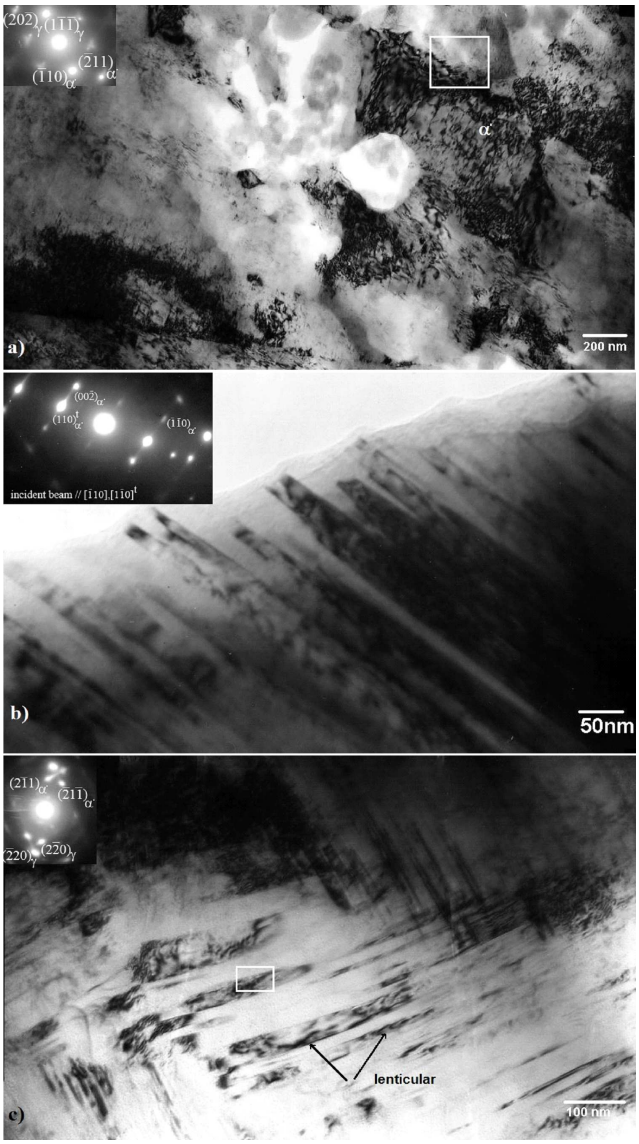

Fig. 2. Bright field TEM micrograph of thermally induced martensite plates and electron diffraction pattern: (a) lenticular martensite in Fe–30%Ni–0.8%Ti alloy, (b) Fe–30%Ni–1.8%Ti alloy, and (c) Fe–30%Ni–2.6%Ti alloy.

orientation relation which corresponds to a typical K–S type relation. In addition to these relationships, Fig. 2b and c illustrates bright field electron micrographs of lenticular martensite plates formed in Fe–30%Ni–1.8%Ti and Fe–30%Ni–2.6%Ti alloys. Crystallographic analyses have shown that martensite twinning have occurred in $\langle 110 \rangle_{\alpha'}$ directions (in Fig. 2b). Figure 2c has an obvious similarity to Fig. 2b. Although the absence of austenite prevents us from determining the variant of the observed martensite plate, we can determine the twin system to be $\{1\ 1\ 2\}_{\alpha'}\langle 111 \rangle_{\alpha'}$ based on the diffraction pattern in Fig. 2c [18–21].

3.3. DSC analysis

The M_s temperatures of thermal induced martensite with –41, –62 and –76 °C are depicted in Fig. 3a–c for $x = 0.8\%$, 1.8%, and 2.6% Ti, respectively. Temperatures decreased as Ti concentration increased. The results obtained are not different from that found by Kaufman [22] for Fe–30%Ni. Kaufman [22] has found the start temperature of martensite and austenite as –42 °C and 335 °C, respectively, and the ending temperature of austenite as 420 °C for Fe–30%Ni. According to these results it can be concluded that the Ti element serves as austenite stabilizer.

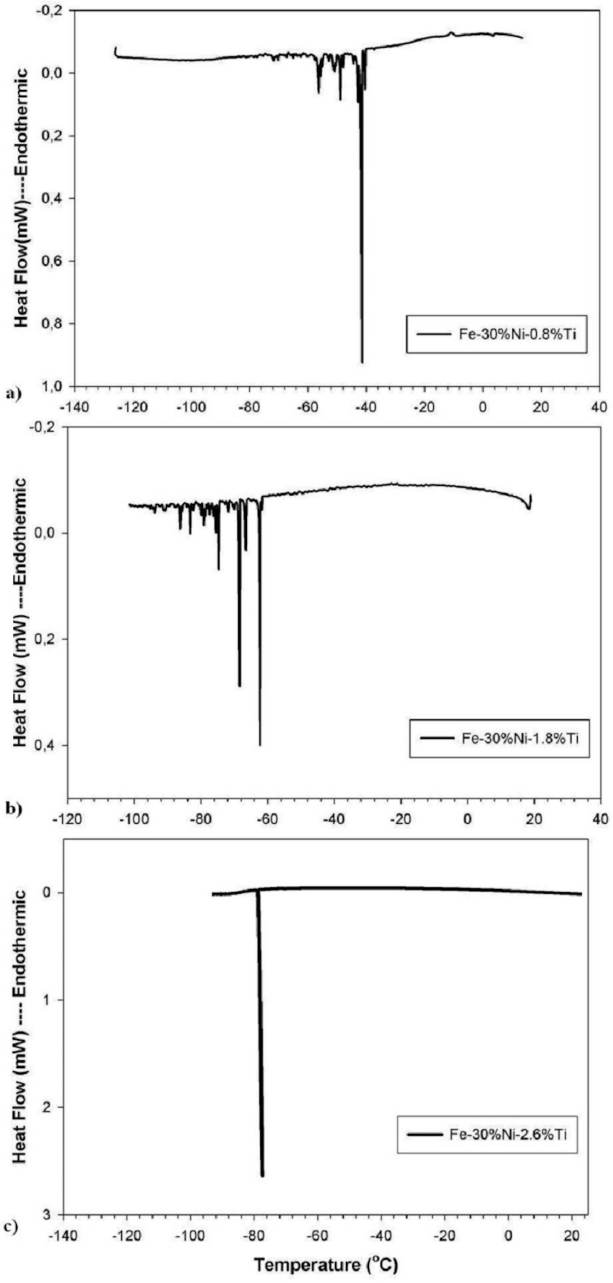

Fig. 3. DSC result of Fe–30%Ni–x%Ti alloys.

3.4. Mössbauer Observations

The magnetic characters of the austenite and martensite phases were examined by using the Mössbauer spectroscopy. Observations of these alloys revealed that the austenite phase is paramagnetic (single peak), and the martensite phase shows a magnetical order (see Fig. 4).

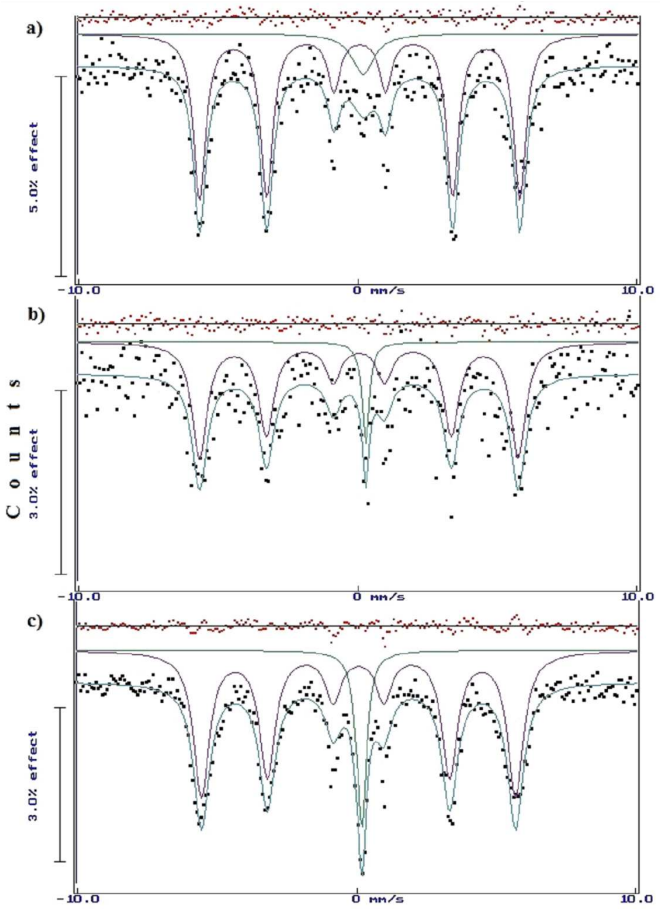

Fig. 4. Room temperature Mössbauer spectra of (a) Fe–30%Ni–0.8%Ti alloy, (b) Fe–30%Ni–1.8%Ti alloy, and (c) Fe–30%Ni–2.6%Ti alloy.

In this figure, the sextets belong to ferromagnetic $\alpha\prime$-martensite phase as the paramagnetic singlets can be ascribed either to γ-austenite phase. The results show that paramagnetic→ferromagnetic ordering also occurs along with $\gamma \rightarrow \alpha\prime$ martensitic transformation in the alloys. In addition, Fig. 4 exhibits that ferromagnetic sextet area decreases as Ti content increases. Thus, the paramagnetic–ferromagnetic ordering of the Fe–30%Ni–x%Ti alloys gradually decreases. It stems from changing of martensite structure. Changes of hyperfine magnetic field H and isomer shift δ have been obtained by Normos-90 fitting program. The Mössbauer parameters, such as δ and H, along with the calculated volume fraction of phases, are shown in Table I. The volume sizes of the martensite crystals formed were found in this section by obtaining the Mössbauer spectra of austenite and martensite phases. Then, athermal conversion has taken place in the liquid nitrogen for the paramagnetic austenite phase, and the Mössbauer spectra were obtained. Internal magnetic field diminishes with the addition of Mo or Si reported earlier study in Fe-based alloys [23]. Furthermore, the decrease in the H indicates a decrease in the magnetic moment [24] which can be attributed to an increase in the electron transfer to the unfilled $3d$ bands [25]. In our previous similar study on Mo concentrations in Fe–30%Ni–x%Mo (x = 0.8, 1.8, and 2.6) alloys, a nearly smooth line was obtained for the variation in H and δ [10]. The change in H and δ depending on the Mo and Ti ratios was illustrated graphically in Fig. 5 and Fig. 6, respectively. For x = 1.8, there was

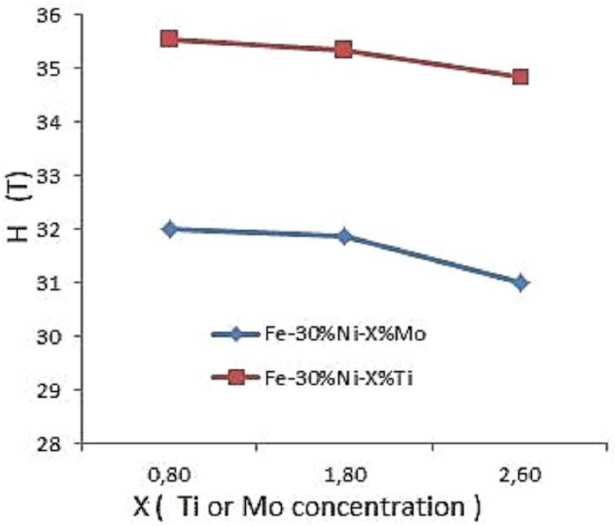

Fig. 5. The variation of H with Ti and the Mo concentration.

a meaningful decrease in δ, but for other concentrations (x = 0.8 and x = 2.6), δ showed no appreciable variation. The decrease of δ at x = 1.8 could be due to the migration of Ti, which reduces the s-electron density to a minimum value.

TABLE I

Mössbauer parameters of the alloys (A — austenite phase, M — martensite phase, δ_M — isomer shift of martensite phase, δ_A — isomer shift of austenite phase and H(T) — internal magnetic field).

Alloys	δ_M [mm/s]	δ_A [mm/s]	%M	%A	H(T)
Fe–30%Ni–0.8%Ti	0.274±0.001	0.040±0.010	91.44	8.56	35.53±0.05
Fe–30%Ni–1.8%Ti	0.190±0.073	0.070±0.006	91.39	8.61	35.34±0.13
Fe–30%Ni–2.6%Ti	0.171±0.001	0.070±0.005	85.91	14.09	34.84±0.04

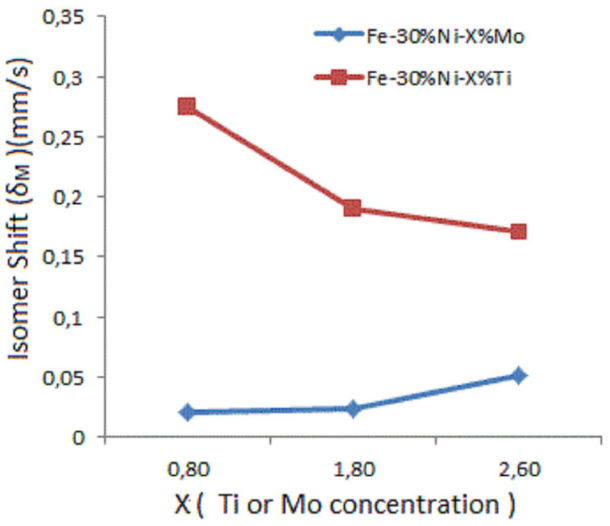

Fig. 6. The variation of δ_M (isomer shifts) with Ti and Mo concentration.

4. Conclusions

This paper studied the effects of Ti concentration on the magnetic properties and the microstructures of Fe–30%Ni–x%Ti alloys. Microstructure analysis revealed that as Ti concentration increased, the rate of martensite structure decreased in SEM micrograph. From the TEM observation and electron diffraction analysis in Fe–30%Ni–x%Ti alloys, it was seen that the formation of thermally induced α' lenticular martensite crystal exhibits the Kurdjumov–Sachs (KS) type relationship. The M_s temperature of thermal induced α' martensite was determined as 41 °C, 62 °C, and 76 °C in the alloys with 0.8%, 1.8%, and 2.6% Ti concentration, respectively. The Mössbauer studies have shown that Ti substitution greatly affects the magnetic properties of Fe–30%Ni–x%Ti alloys. The value of the H and isomer shifts δ decreased with increasing Ti ratio. In thses alloys, the amount of α' lenticular martensite which is the source of the internal magnetic field is found to be related to the Ti ratio.

References

[1] Z. Nishiyama, *Martensitic Transformation*, Academic Press, New York 1978.

[2] A. Shibata, T. Murakami, S. Morito, T. Furuhara, T. Maki, *Mater. Trans.* **49**, 1242 (2008).

[3] A. Shibata, S. Morito, T. Furuhara, T. Maki, *Scr. Mater.* **53**, 597 (2005).

[4] K. Bhattacharya, S. Conti, G. Zanzotto, J. Zimmer, *Nature* **428**, 55 (2004).

[5] L. Malet, S. Godet, *Scr. Mater.* **102**, 83 (2015).

[6] T. Maki, *Mater. Sci. Forum* **56-58**, 157 (1990).

[7] L. Zhang, T. Ohmura, A. Shibata, K. Tsuzaki, *Mater. Sci. Eng. A* **527**, 1869 (2010).

[8] A.I. Medved, V.G. Gorbach, *Metallofizika* **3**, 62 (1982).

[9] H. Gungunes, E. Yasar, M. Dikici, *Int. J. Min. Met. Mater.* **18**, 192 (2011).

[10] E. Yasar, H. Gungunes, A. Kilic, T.N. Durlu, *J. Alloys Comp.* **424**, 51 (2006).

[11] H. Gungunes, E. Yasar, A. Kilic, T.N. Durlu, *Mater. Sci. Tech.* **23**, 975 (2007).

[12] M. Mizrahi, A.F. Cabrera, S.M. Cotes, S.J. Stewart, R.C. Mercader, J. Desimoni, *Hyperfine Interact.* **156-157**, 541 (2004).

[13] A. Das, *J. Magn. Magn. Mater.* **361**, 232 (2014).

[14] S.M. Cotes, A.F. Cabrera, L.C. Damonte, R.C. Mercader, J. Desimoni, *Hyperfine Interact.* **141-142**, 409 (2002).

[15] J. Martinez, G. Aurelio, G. Cuello, S.M. Cotes, A.F. Guillermet, J. Desimoni, *Hyperfine Interact.* **16**, 221 (2005).

[16] P. Novak, V. Chlan, *Phys. Rev. B* **81**, 174412 (2010).

[17] M. Birsan, B. Fultz, L. Anthony, *Phys. Rev. B* **55**, 11502 (1997).

[18] J.S. Bowles, J.K. Mackenzie, *Acta Metall.* **2**, 129 (1954).

[19] J.K. Mackenzie, J.S. Bowles, *Acta Metall.* **2**, 138 (1954).

[20] M.S. Wechsler, *Acta Metall.* **7**, 793 (1959).

[21] T. Maki, S. Shimooka, I. Tamura, *Metall. Trans.* **2**, 2944 (1971).

[22] L. Kaufman, Ph.D. Thesis, MIT, 1958.

[23] Y.U.L. Rodionov, G.G. Isfandiyarov, V.N. Zambrzhitskiy, *Phys. Met. Metall.* **49**, 94 (1980).

[24] P. Panissod, J. Durand, J.I. Budnick, *Nucl. Instrum. Methods* **199**, 99 (1982).

[25] K. Yamauchi, T. Mızoguchi, *J. Phys. Soc. Jpn.* **39**, 541 (1975).